

# Dynamic Drive Performances of the Bionic Suction Cup Actuator Based on Shape Memory Alloy

Yunhao Ge<sup>1</sup>, Jihao Liu<sup>2</sup>, Bin Li<sup>2</sup>, Huihua Miao<sup>1</sup>, Weixin Yan<sup>1(✉)</sup>,  
and Yanzheng Zhao<sup>1</sup>

<sup>1</sup> Robotics Institute of Shanghai Jiao Tong University, Shanghai 200240, China  
{gyhandy, xiaogu4524, yzh-zhao}@sjtu.edu.cn

<sup>2</sup> State Key Laboratory of Mechanical System and Vibration, Shanghai Jiao Tong University,  
Shanghai 200240, China

**Abstract.** This paper proposes a design of SMA-based bionic suction cup actuator, the core of which is that the bias spring cooperates with the SMA spring to produce a displacement at the varying temperature caused by the drive current. To characterize the dynamic drive performance of the actuator, the thermodynamic model is established by the constitutive model of SMA material of Tanaka series. The simulation model for the bias SMA spring actuator in MATLAB/SIMULINK is built. Moreover, the effects of different load and different driving environment on the displacement of SMA actuator as well as the corresponding reaction time are investigated. The steady displacement response enlarge with the drive current increasing, while the load readjusts the initial deformation of the actuator and also enlarges the final steady shearing displacement. Further, based on the actuator driving performance, the adsorption characteristics of the bionic suction cup are studied and verified experimentally.

**Keywords:** Bionic suction cup · SMA spring actuator · Dynamic drive performance · Adsorption characteristics

## 1 Introduction

Micro bionic suction cup actuator design mainly considers the bionic, driving characteristics and efficiency. Vacuum pressure suction actuated by the tissue's elastic deformation has relatively excellent stability and adhesion performance [1], and is the easiest to be imitated. Bionic suction cup drives need to have a similar muscle nature, not only have a large output displacement, but also should have the appropriate drive frequency and weight ratio.

Considering the new functional materials applied in bionic suction cup, because the output power of the ion-exchange polymer metal composite(IPMC) driver is very small [2], while the drive voltage of electroactive polymer (EAP) is as high as the kilovolt [3], compared with piezoelectric actuator, the amount of deformation of the SMA drive is much greater. Especially SMA actuators have the advantages of low driving voltage, high driving force, no noise and high weight ratio. This paper adopts the SMA spring actuator driving the miniature bionic suction cup.

The spring-like SMA actuator is capable of generating the larger strain of which the bionic suction cup takes advantage to generate vacuum pressure. The SMA actuator's principles are on the basis of the shape memory effect which generates the force and displacement in the process of martensitic phase transformation as the temperature changes [4].

The relationship between the force and deformation of the SMA actuator is no linear [5]. It is hard to establish an accurate mathematical model, while the study methods of the dynamic characteristics are different under multi-driving environment. However, the dynamic performance of SMA actuators under different currents and different loads directly affects the reliability and the performance of bionic suction cup. This paper focuses on the driving performance of bidirectional SMA actuators and experiments on the adsorption characteristics of micro-bionic suction cup based on SMA actuator.

## 2 The Thermo-Dynamical Model of SMA Spring

In order to estimate the adsorption performance of bionic suction cup actuated by SMA, it's essential to set up the theoretical model for the driving performance of SMA actuator. The paper briefly introduces Liang-Rogers constitutive equation of SMA material, then deduces the thermo-dynamical model of SMA spring actuators that reflects the relationship between the output force/displacement and the input current [6].

The martensitic volume fraction ( $\xi$ ) depends on the temperature ( $T$ ) and the stress ( $\sigma$ ) during the process of the phase transformation [7]. Liang founded the dynamic model using sine basis functions for the phase transformation of the SMA material. When SMA spring cools, the martensitic phase transformation yields:

$$\xi = \frac{1 - \xi_A}{2} \cos[a_M(T - M_f) + b_M\sigma] + \frac{1 + \xi_A}{2} \quad (M_f + \frac{\sigma}{C_M} \leq T < M_s + \frac{\sigma}{C_M}) \quad (1)$$

While SMA spring is being heated, the austenitic phase transformation yields:

$$\xi = \frac{\xi_M}{2} \{ \cos[a_A(T - A_s) + b_A\sigma] + 1 \} \quad (A_s + \frac{\sigma}{C_A} \leq T < A_f + \frac{\sigma}{C_A}) \quad (2)$$

$\xi_A$  and  $\xi_M$  respectively refer to the initial martensitic volume fraction in the austenitic and martensitic phase transformation;  $a_A$ ,  $a_M$ ,  $b_A$  and  $b_M$  are material constants,  $M_s$  and  $M_f$  are the initial and final temperature in the martensitic phase transformation;  $A_s$  and  $A_f$  are the initial and final temperature in the austenitic phase transformation;  $C_A$  and  $C_M$  are material constants.

The equations listed above reflect the constitutive model of the SMA wire under the one-dimension tension or compression, but there exist sheering stress  $\tau$  and sheering strain  $\gamma$  in the spring's deformation process. We can obtain the new one under the shearing condition [8].

$$\tau - \tau_0 = G_{sma}(\gamma - \gamma_0) + \frac{\Theta}{\sqrt{3}}(T - T_0) + \frac{\Omega}{\sqrt{3}}(\xi - \xi_0) \quad (3)$$

The equivalent stress equation in the elastic-plastic mechanics  $\sigma = \sqrt{3}\tau$ ; the equivalent strain equation  $\varepsilon = \sqrt{3}\gamma$ . Suppose that the actuator's load force is  $F_{sma}$ , the shear displacement is  $y$ , the number of active coils is  $n$ , spring diameter and wire diameter are  $D$  and  $d$  respectively, then according to the coil springs theory, we can deduce the shearing stress  $\tau$  and shearing strain  $\gamma$  of the SMA spring heating:

$$\gamma = \frac{8F_{sma}D}{G_{sma}\pi d^3} \quad \tau = \frac{8F_{sma}D}{\pi d^3} \quad (4)$$

Suppose there is neither stress nor strain in the spring at the initial moment, we can obtain:

$$y = \frac{\pi n D^2}{d G_{sma}} \tau - \frac{\pi n D^2}{d G_{sma}} \frac{\Theta}{\sqrt{3}}(T - T_0) - \frac{\pi n D^2}{d G_{sma}} \frac{\Omega}{\sqrt{3}}(\xi - \xi_0) \quad (5)$$

Uniting Eqs. (3) and (5), we can obtain the simplified relationship among the load force ( $F_{sma}$ ), the shear displacement ( $y$ ), the martensitic volume fraction ( $\xi$ ) and the temperature ( $T$ ):

$$F_{sma} = \frac{d^4 G_{sma}}{8nD^3} y + \frac{\pi d^3}{8D} \frac{\Theta}{\sqrt{3}}(T - T_0) + \frac{\pi d^3}{8D} \frac{\Omega}{\sqrt{3}}(\xi - \xi_0) \quad (6)$$

The SMA actuator responding to the temperature change generates the force and displacement, which can be caused by heating and cooling. The electric heating devices is easy to control with the external power supplying, while the air cooling being realized through the heat exchange with the environment. To create the micro bionic suction cup, this paper assembles the SMA actuator with the electric heating and the air cooling. Figure 1 illustrates the heat transfer process, in which the heat actuating the SMA spring is Joule heat that dissipates through conduction, convection and radiation. Almost ninety percent of the heat passes into the air in convection, and the remaining mainly radiates, while the heat by conduction is negligible.

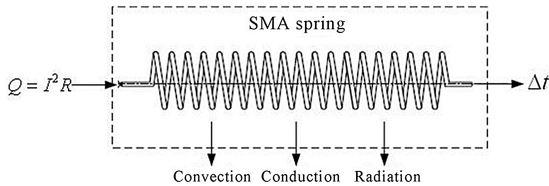


**Fig. 1.** SMA spring's heat transfer analysis

We can obtain the heat diffusion equation of SMA actuator during the process of the temperature change:

$$\frac{\partial t}{\partial \tau} = \frac{h}{\rho c} \left( \frac{\partial^2 t}{\partial x^2} + \frac{\partial^2 t}{\partial y^2} + \frac{\partial^2 t}{\partial z^2} \right) + \frac{\dot{\Phi}}{\rho c} \quad (7)$$

In the equation above,  $t$  denotes the SMA's temperature;  $\tau$  denotes time;  $c$  denotes the specific heat;  $\rho$  denotes the density;  $h$  denotes the heat conductivity coefficient and  $\Phi$  denotes the heat intensity respectively. Since SMA model conforms the simplified lumped parameter conditions, the heat conduction has nothing to do with the model's temperature and the coordinate. The Eq. (7) can be simplified [9]. The heat intensity in the electric heating process is:

$$\dot{\Phi}_t = \frac{\Delta \Phi_v}{\Delta V} = \frac{I^2 R}{V} \quad (8)$$

Here  $R$  and  $V$  are SMA material internal resistance and volume respectively. The negative heat-intensity in the heat-dissipation is:

$$\dot{\Phi}_w = \frac{\Delta \Phi_w}{\Delta V} = \frac{hA(t - t_\infty)}{V} \quad (9)$$

$t_\infty$  is the environment temperature;  $A$  is the heat radian surface area of the SMA actuators. Based on the Eqs. (8) and (9), we can obtain the temperature change of the SMA actuator heated by the electric component:

$$\rho c V \frac{dt}{d\tau} = I^2 R - hA(t - t_\infty) \quad (10)$$

In the actuator's natural cooling process, the first stem of the upper equation does not exist any longer. Given the driving current is  $I$ , we can obtain the martensitic volume fraction of the phase transformation at the current temperature determined by Eq. (10). Then we can calculate the spring's shear force and displacement based on the thermodynamic model of the SMA spring.

### 3 Dynamic Driving Performance of Two-Way SMA Spring Actuator

The two-way SMA actuators must have the capability to execute double action reciprocating in order to generate or release the vacuum pressure. The actuators equipped with the SMA spring is of the two-way shape memory effect which extends when heating and contracts when cooling. In terms of the types of the bias elements, the two-way SMA actuators can be divided into the bias one using the conventional spring and the differential one that are equipped with additional SMA spring that produces the restoring force [10]. The paper estimates and analyzes the driving performance of the bias SMA spring actuator by theoretical methods and experiment.

Based on the principles above, the paper demotes a novel bias spring actuator as shown in Fig. 2, which is made up of the outer shell, the guide rod, the support plate, the movable part, the bias spring and the SMA spring that together drive the guide rod bidirectionally linear moving subject to the alternative temperature.

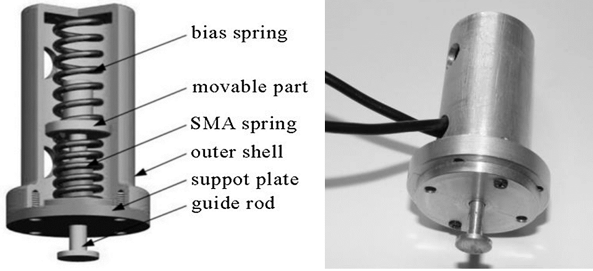


**Fig. 2.** Design of the bias SMA spring actuator

Suppose the length of SMA spring and bias spring are  $l_s$  and  $l_b$  in the natural state with no load, then the sum length of two springs assembled in the outer shell is compressed to  $l$ ; the elastic modulus of the bias spring is  $K_b$ . The springs' deformation are  $\Delta l_s^i$  and  $\Delta l_b^i$  respectively at the initial moment. When subjected to variable temperature, the SMA spring and the bias spring will produce the shearing displacements that is respectively represented by sign  $\Delta l_s^h$  and  $\Delta l_b^h$ . And the shearing displacements meet the geometrical relationship all the time:

$$\Delta l_b^{i/h} = (l_b + l_s) - (l + \Delta l_s^{i/h}) \quad (11)$$

At the initial moment, the SMA spring generates shear force  $F_s^i$  that is equal to bias spring force  $F_b^i$ , hence the SMA spring is only of martensite at the atmospheric temperature, and we can obtain:

$$\frac{d^4 G_{sma}}{8knD^3} \Delta l_s^i = F_s^i = F_b^i = K_b \Delta l_b^i \quad (12)$$

Based on Eqs. (11) and (12), we can obtain the shearing displacement of the SMA spring and the bias spring  $\Delta l_s^i$  and  $\Delta l_b^i$  at the initial state. In the process that the two-way actuator is subject to the alternative temperature, the SMA spring's shearing force  $F_s^h$  and the bias spring's one  $F_b^h$  yield:

$$\frac{d^4 G_{sma}}{8knD^3} \Delta l_s^h + \frac{\pi d^3}{8kD} \frac{\Theta}{\sqrt{3}} (T - T_0) + \frac{\pi d^3}{8kD} \frac{\Omega}{\sqrt{3}} (\xi - \xi_0) = F_s^h = F_b^h = K_b \Delta l_b^h \quad (13)$$

The spring's temperature  $T$ , martensitic volume fraction  $\xi$  and the shearing modulus  $G_{sma}$  are introduced into Eq. (13), in combination with Eq. (11), we can obtain the

shearing displacement from the SMA spring and bias spring are  $\Delta l_s^h$  and  $\Delta l_b^i$  respectively. In the operation process, the shearing displacement  $\Delta l$  generated by the bias spring actuator is:

$$\Delta l = \Delta l_s^i - \Delta l_s^h \quad (14)$$

According to the theoretical model above, the paper founds the simulation model about the bias spring actuator in MATLAB/SIMULINK as shown in Fig. 3. Table 1 lists the feature parameters in the simulation about the SMA spring and the bias spring. We heated the SMA spring driven by the DC regulated power supply in the experiments. The simulation result in the SIMULINK was compared in terms of the records of the temperature change and the shearing displacement under the variable loads and the driving currents, aiming to prove the validity of the theoretical model for the bias SMA spring actuators.

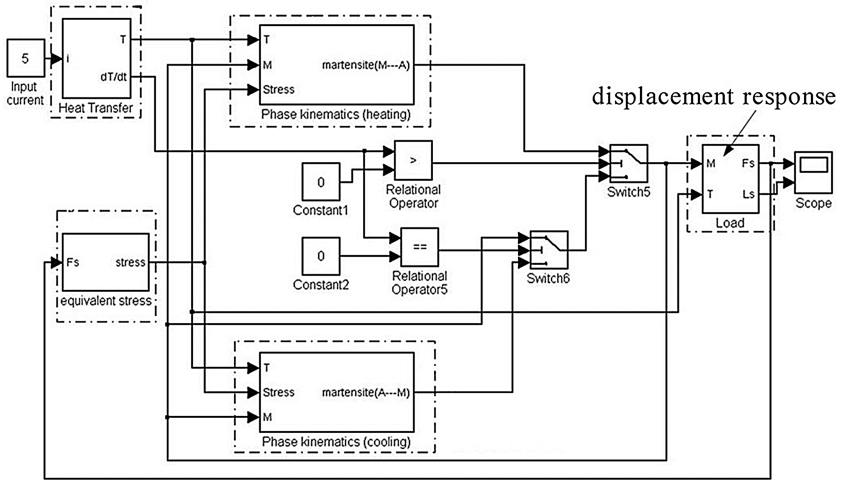


**Fig. 3.** Simulation model of bias SMA spring actuator

As shown in Fig. 4(a), the dynamic curve reflects the simulation temperature of the SMA Spring heated under various driving currents. At the beginning, the velocity of the spring's temperature change accelerates in accordance with the heating current at the same case of ambient temperature and heat dissipation condition. The SMA spring's temperature tends to reach a steady value though a period of thermal equilibrium. In general, the larger the heating current is, the longer it takes to gradually return to the atmosphere temperature by air cooling.

**Table 1.** The feature parameters of bias SMA spring actuator

SMA spring				Bias spring	
Density $\rho$ (kg/m <sup>3</sup> )	6500	Specific heat $c_p$ (J/Kg <sup>°C</sup> )	320	Elastic modulus $k_b$ (N/m)	850
Resistance $R$ ( $\Omega$ )	0.15	Heat conduction coefficient $h$ (W/m <sup>2</sup> °C)	120	Initial length $l_b$ (mm)	24
Ambient temperature $T_{00}$ (°C)	20	Martensitic elastic modulus $D_M$ (Pa)	28e9		
Austenitic elastic modulus $D_A$ (Pa)	75e9	Poisson's ratio $\mu_{SMA}$	0.33		
The initial temperature of the martensitic phase transformation $M_s$ (°C)	40	The final temperature of the martensitic phase transformation $M_f$ (°C)	20		
The initial temperature of the austenitic phase transformation $A_s$ (°C)	40	The final temperature of the austenitic phase transformation $A_f$ (°C)	60		
Material constant $C_M$ (Pa/°C)	10.3e6	Material constant $C_A$ (Pa/°C)	10.3e6		
Coefficient of thermal expansion $\Theta$ (Pa/°C)	0.55e6	Active coil number(n)	9		
Spring's diameter $D$ (mm)	7.3	Wire diameter $d$ (mm)	1.3		

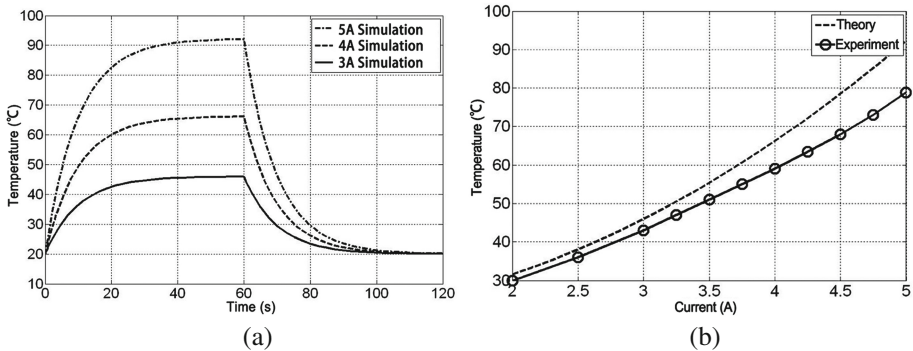


**Fig. 4.** (a) Temperature response of SMA spring (b) Relationship between stable temperature and actuating currents

Figure 4(b) illustrates that the SMA spring can be subject to a certain steady temperature to the driving current in both practical experiment and simulation, which conforms the SMA spring's simulation models. Nevertheless, there exists some error between the theoretical simulation and the experimental that mainly results from the constitutive model error and the feature parameter error.

Figure 5 shows the displacement response of the bias SMA spring actuator stimulated by different amplitude current whose duty cycle is 0.5 in 160 s. Subject to 4A in the driving current with no load, the spring generates the shearing displacement in the simulation that is almost close to the experiment result. It indicates the theoretical model of SMA spring and bias actuator are valid.

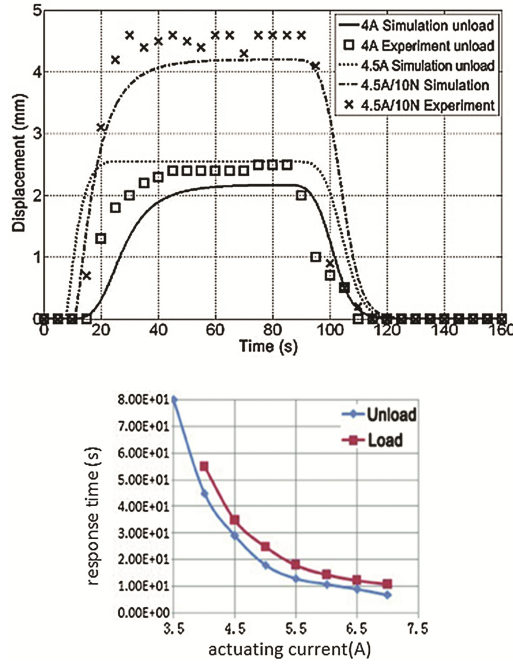


**Fig. 5.** (a) Displacement response of the bias SMA spring actuator; (b) Relationship between response time and actuating currents

Given that the constant driving current is 4A, the SMA spring starts to generate the shearing displacement at 15 s; when the heating temperature gradually exceeds the starting point of austenitic phase transformation, the SMA spring's equivalent elastic modulus will become stronger, which will extend to push the guide rod. At the end of the austenitic phase transformation, shearing displacement and the equivalent elastic modulus are stable and the guide rod will no longer move outward. When the driving current is larger, SMA spring's temperature will reach a much higher stable point more rapidly, so does the actuator's displacement. When SMA spring is in the air cooling process, the springs' shearing displacement gradually decreases. Based on the simulation and experiment result in the case that two-way actuator is loaded with nothing, we can find that the driving current has no effect on the spring's shearing restoration generated from the shearing deformation of the bias spring mainly.

According to the observation, the dynamic response curve of the shearing displacement is subject to variable loads. Comparing to the cases under various loads in Fig. 5(a), it will take the spring longer heating period to generate the shearing displacement than one with no loads in the same conditions. Due to the fact that the stress has an effect on the martensitic phase transformation of the SMA material, the starting point of austenitic phase transformation is higher under the load. So it will cost much longer time to preheat to generate obvious shearing displacement. Meanwhile, the load readjusts the initial



deformation of the bias spring and the SMA spring and still enlarges the final steady shearing displacement.

Under the case that the load is 0 and 10 N respectively, the dynamic relationship curve mapping between the stable response period and the driving current are derived from the practical experiment as shown in Fig. 5(b). Given the driving current is 4A, the actuator that loads 10 N will generate 4.5 mm of the steady shearing displacement in 35 s. The experiment indicates the overload that has the destructive effect on the shape memory effect will prevent the SMA spring from being restored to the initial state, which will shorten the two-way's mechanical lifetime in this circumstance.

Figure 6 illustrates the relationship between stable displacement and the driving current in two cases of different loads. Given the temperature of the SMA spring is close to the atmosphere in the initial state, the actuator with no load will start to generate the shearing displacement as long as the driving current is over 2.4A. The same actuator with a certain load must be applied over 3A of driving current to generate the displacement. With the increasing driving current on the SMA spring, the stable value of the shearing displacement gradually enlarges, while the current is over the ultimate point, the steady displacement stays the same. As shown in Fig. 6, the driving current applied to the actuator unloaded is over 4A, the maximum stable shearing displacement is about 2.5 mm, which means SMA spring has reached the stable ultimate point that is the end of the austenitic phase transformation. When the driving current on the actuator with the load of 10 N reaches 4.5A, the ultimate steady displacement will be 4.5 mm.

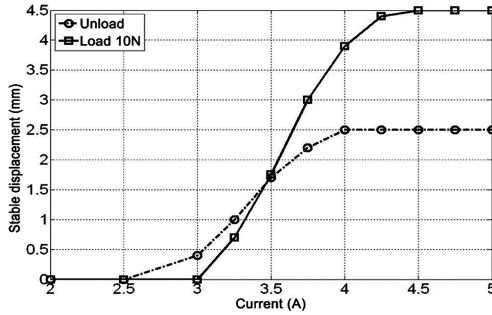
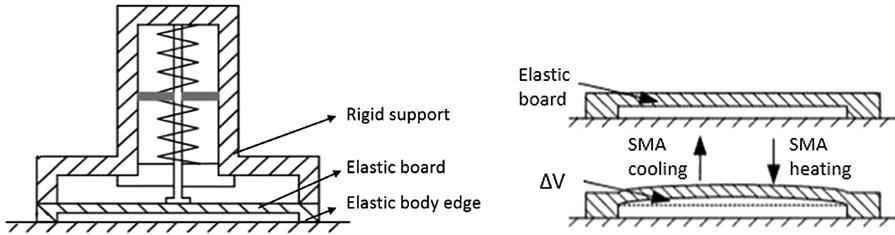


Fig. 6. Relationship between stable displacement and actuating currents

#### 4 Experimental Investigation of the Adsorption Characteristics of Bionic Suction Cup

The dynamic response of the SMA actuator includes the generation and disappearance of vacuum pressure. Vacuum pressure requirements are quickly generated or canceled to match the footwall movement of the climbing robot. As Fig. 7 shows, the lower end of the actuator is connected with the elastomer plate to form a bionic suction cup prototype.



**Fig. 7.** Application of SAM actuators for the bionic suction cup

To test the vacuum pressure response of the prototype under different drive current, the full 5 V bias pressure sensor MPX5100 with the range of 100 kPa was installed at the lower surface of the adsorption surface, and was drilled on the suction surface, so the inlet of the vacuum pressure sensor communicates with the air cavity of the prototype. A constant current source has been used to heat the SMA actuator, and the oscilloscope was used to record the vacuum pressure response in the bionic suction cup, the test equipmenting is shown in Fig. 8.

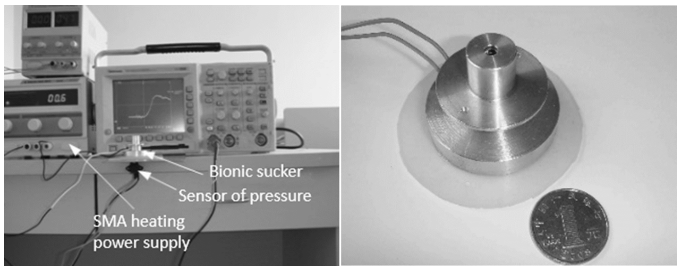


**Fig. 8.** Experimental equipments of vacuum pressure response testing

Figure 9(a) shows the response curves for the generation of vacuum pressure under different drive currents. When the drive current is constant, the response curve is similar to that of the biased SMA spring actuator output displacement. Under the drive current 4.75A, the bionic suction cup can produce the maximum vacuum pressure of about 14000 Pa, with the peaking time of 25 s. As the drive current increases, the steady-state vacuum pressure will also increases, while the peaking time of the maximum vacuum pressure value decreases. Bionic suction cup can almost reach the same steady-state vacuum pressure under the drive current of 4.5A or 4.7A, which illustrates that the SMA spring undergoes a complete austenite transformation under the current over 4.5A, and both the output displacement and the vacuum pressure can not increase with increasing current.

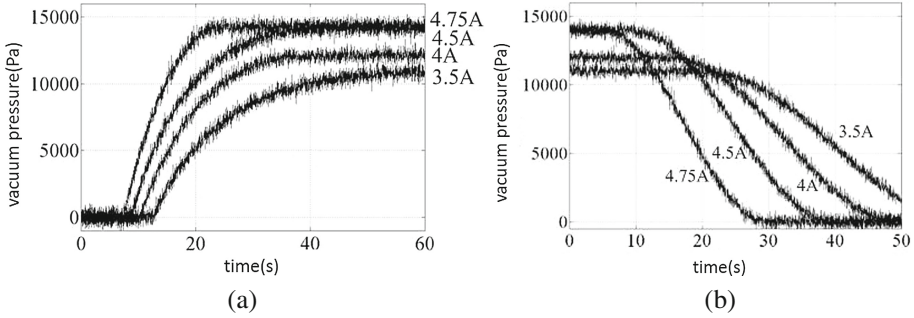


**Fig. 9.** (a) Waveform of vacuum pressure's generation; (b) Waveform of vacuum pressure's cancelling

To study the response curve during the disappearance process: firstly, the vacuum pressure within the suction cup achieve steady-state value under different drive current. Then the SMA spring heating current should be cancelled, and the process of suction cup vacuum pressure response curve in Fig. 9(b) should be recorded. With the increase of the drive current, the vacuum pressure cancellation time is slightly reduced, but from the overall point of view, the drive current has little effect on the cancelling process of vacuum pressure. Because when the drive current is larger, the amount of deflection of the bias spring increases, resulting in a greater return force. Meanwhile, SMA spring austenite phase change is deeper, the force applied to the bias spring is also larger; and the SMA spring heat dissipation conditions are exactly the same, with about 20 s disappears time.

## 5 Conclusions

This paper uses the SMA spring actuator to drive the micro bionic suction cup. To investigate the driving performance of the SMA actuator, the paper deduces the thermodynamic model for SMA spring based on the constitutive model, and estimates the dynamic driving performance of the SMA bias actuator by simulation and experiments, which prove the validity of theoretical model. When drive current is applied to the SMA spring actuator, the actuator will generate the increasing displacement linearly with the temperature arising that will reach a steady ultimate point in the case that there exists thermal equilibrium between the SMA and the air. The stronger the driving current is, the higher the temperature of the spring is, and the larger the steady displacement response will be. Meanwhile, the load has profound impact on the steady displacement and respond time of the actuator. Finally, the vacuum pressure response curve of bionic suction cup under different current is similar to that of the biased SMA spring actuator output displacement, which verifies the feasibility of the design.

**Acknowledgments.** This work is supported by the National Natural Science Foundation of China under Grant No. 51475305 and 61473192.

## References

1. Nachtigall, W.: Animal attachments: minute, manifold devices. biological variety-basic physical mechanisms-a challenge for biomimicking technical stickers. In: Bionik. Springer, Berlin, Heidelberg. pp. 110–111 (2005)
2. Kim, B., Ryu, J., Jeong, Y. et al. A ciliary based 8-legged walking micro robot using cast IPMC actuators. In: Proceedings of the IEEE International Conference on Robotics and Automation. Taipei. pp. 2940–2945 (2003)
3. Walker, I.D., Dawson, D.M., Flash, T., et al. Continue robot arms inspired by cephalopods. In: Proceedings of the SPIE Unmanned Ground Vehicle Technology, vol. 5840, Orlando, USA. pp. 303–314 (2005)
4. Huang, W.: Shape memory alloys and their application to actuators for deployable structures. University of Cambridge Department of Engineering, England (1998)
5. Huang, W.: On the selection of shape memory alloys for actuators. In: Materials & Design, vol. 23, Issue 1, pp. 11–19 (2002)
6. Liang, C., Rogers, C.A., et al.: A multi-dimensional constitutive model for shape memory alloys. J. Eng. Math. **26**(3), 429–443 (1992)
7. Mammanno, Scirè G., Dragoni, E.: Effects of loading and constraining conditions on the thermomechanical fatigue life of NiTi shape memory wires. J. Mater. Eng. Perform. **23**(7), 2403–2411 (2014)
8. Hu, B.: Bio-inspired miniature suction cups actuated by shape memory alloy. Int. J. Adv. Rob. Syst. **6**(3), 151–160 (2009)
9. Yu, H.: Rigid/compliant coupling wheeled micro robot based on shape memory alloy. Shanghai Jiao Tong University, Shanghai (2006)
10. Yang, B., Zhang, X., Yan, X.: Relationship between bias spring parameters and output performances of SMA actuators. J. Beijing Univ. Aeronaut. Astronaut. **41**(4), 707–712 (2015)

Intelligent Robotics and Applications

10th International Conference, ICIRA 2017, Wuhan,  
China, August 16–18, 2017, Proceedings, Part I

Huang, Y.; Wu, H.; Liu, H.; Yin, Z. (Eds.)

2017, XXXIII, 887 p. 565 illus., Softcover

ISBN: 978-3-319-65288-7